Journal of Applied Polymer Science

# Preparation, Structure, and Properties of Chitosan/Cellulose/Multiwalled Carbon Nanotube Composite Membranes and Fibers

**Wenjun Xiao,[1,2,3] Tinghua Wu,[1] Jiajian Peng,[2] Ying Bai,[2] Jiayun Li,[2] Guoqiao Lai,[2] Ying Wu,[1] Lizong Dai[3]**

[1]Institute of Physical Chemistry, Zhejiang Normal University, Jinhua 321004, China
[2]Key Laboratory of Organosilicon Chemistry and Material Technology of Ministry of Education, Hangzhou Normal University, Hangzhou 310012, China
[3]Key Laboratory of Fire Retardant Materials of Fujian Province, College of Materials, Xiamen University, China
Correspondence to: T. Wu (E-mail: thwu@zjnu.cn) or J. Peng (E-mail: jjpeng@hznu.edu.cn)

**ABSTRACT:** Binary ionic liquids (ILs), 1-butyl-3-methylimidazolium chloride and 1-H-3-methylimidazolium chloride, were developed to dissolve chitosan and cellulose and disperse multiwalled carbon nanotubes (MWCNTs). The resulting mixed paste could be used to prepare chitosan/cellulose/MWCNT composite membranes and fibers. Fourier transform infrared spectroscopy, wide-angle X-ray diffraction, thermogravimetric analysis, scanning electron microscopy, tensile testing, and conductivity measurements were used to evaluate the structure and properties of the composite materials and the effect of the incorporation of MWCNTs at various loadings. The characterization results indicate that the incorporation of MWCNTs improved the comprehensive performances of the composite materials, and the best loading of MWCNTs was 4 wt %. This IL dissolution method is a green and feasible method for preparing chitosan/cellulose/MWCNT composite membranes and fibers and will provide beneficial references for the preparation of similar materials. © 2012 Wiley Periodicals, Inc. J. Appl. Polym. Sci. 000: 000–000, 2012

**KEYWORDS:** cellulose and other wood products; composites; ionic liquids

Received 10 April 2012; accepted 7 July 2012; published online
**DOI: 10.1002/app.38329**

## INTRODUCTION

Chitosan is the second most abundant natural polymer on the earth, consisting of β-(1-4)-2-amino-D-glucose and β-(1-4)-2-acetamido-D-glucose.[1] Chitosan and its derivatives are becoming increasingly important because of their promising properties, including their low toxicity, biocompatibility, biodegradability, and nonantigenicity.[2,3] Accordingly, they are widely used in metal chelating agents, medicine, artificial skin, food additives, antimicrobial agents, adhesives, textiles, and so on.[4,5] It can be easily shaped into fibers, films, hollow fibers, membranes, medical gauze, and wound dressings.[6] However, their poor mechanical properties limit their use in wide-range application. Two methods can solve this problem effectively. One is the blending of chitosan with other polymers. Various polymers, such as poly(vinyl alcohol),[7] poly(*N*-vinyl pyrrolidone),[8] polyaniline,[9] starch,[10] and cellulose[11] and its derivatives,[12] are frequently used to be blended in the chitosan matrix. The other is the incorporation of nanofillers, including silica, clay, and carbon nanotubes (CNTs), which are frequently used to reinforce the chitosan matrix.[13–15] Both methods are commonly used to prepare new polymer materials with improved physicochemical, mechanical, electrical, and thermal properties.

Cellulose, the most abundant natural polymer in nature, is renewable, biodegradable, and biocompatible. Furthermore, cellulose has superior ability of film and fiber formation. Therefore, it is significant to obtain blended materials that combine the properties of chitosan and cellulose. However, because of their large proportion of intramolecular and intermolecular hydrogen bonds, both chitosan and cellulose are difficult to process in solution or as a melt. Generally, *N*-methylmorpholine-*N*-oxide/$H_2O$ system is used as a solvent to prepare chitosan/cellulose blended materials.[11,16] However, the *N*-methylmorpholine-*N*-oxide/$H_2O$ system has some disadvantages, including a demand for high temperature for dissolution, the degradation of chitosan and cellulose, the side effects of the solvent itself without an antioxidant, and its high cost. So it is very necessary to find an effective solvent for chitosan and cellulose. Moreover, the materials formed from the chitosan and cellulose solution have poor mechanical properties, especially a low tensile strength. Therefore, a method for enhancing the mechanical

properties of chitosan/cellulose blends is another problem we considered in this study.

As we know, CNTs are considered an important group of nanomaterials, with a nanometer size, high aspect ratios, extraordinary mechanical strength, and high electrical and thermal conductivity.[17] The extraordinary mechanical and electrical properties of CNTs make them outstanding reinforcing fillers for polymer matrices for the achievement of high performance and multiple functions. To achieve the full reinforcing potential of CNTs in polymers, they must be well dispersed and exhibit good interfacial strength with the matrix. The covalent functionalization of CNTs was reported;[18] strong interfacial strength between the CNTs and polymer matrix was evident, but it impaired some of the important properties of CNTs. This drawback can be prevented with surfactants, but such surfactant-modified CNTs only show moderate enhancements in the mechanical properties.[19,20] This is likely because the addition of surfactants reduces the interaction of the polymer and CNTs.

Recently, ionic liquids (ILs) have attracted great interests in green chemistry because of their high stability, high electrical conductivity, and very low vapor pressure. Pioneer studies by Fukushima et al.[21] showed that single-walled carbon nanotubes can be well dispersed in ILs. This dispersion is most likely due to the adhesion of ILs via a $\pi$ cation/$\pi$ interaction onto the nanotube surface and provides an alternative route for preparing new functional materials and polymer composites containing CNTs. It is worth noting that the inherent properties of CNTs do not change by this method. On the other hand, ILs are promising solvents for the dissolution of polysaccharides such as chitin,[22] chitosan,[23] and cellulose.[24] The resulting homogeneous solution is coagulated to obtain regenerated materials. Thus, chitin membranes,[22,25] chitin fibers,[26] cellulose membrane/fibers,[27] chitin/cellulose blended membranes,[26] and cellulose/multiwalled carbon nanotube (MWCNT) composite fibers[27] can be prepared by this method. In addition, after regeneration, the residual ILs in the coagulation bath can be effectively recovered. Therefore, the IL dissolution method seems to be a promising green process for preparing regenerated biopolymer materials and can overcome the inherent environmental problems.[24] However, few studies have been reported on chitosan materials prepared by the IL dissolution method.

In this work, the binary ILs 1-butyl-3-methylimidazolium chloride (BMImCl) and 1-H-3-methylimidazolium chloride (HMImCl) were used to prepare chitosan/cellulose blended membranes and fibers. MWCNTs were used to reinforce these blended membranes and fibers to obtain the final composite materials. Details of preparation, characterization, thermal stability, mechanical properties, and electrical conductivity of the chitosan/cellulose/MWCNT composite membranes and fibers are also described.

## EXPERIMENTAL

### Materials

Chitosan (deacetylation degree > 90%) and microcrystalline cellulose were purchased from Qingdao Shenyan Chemical Industry Co., Ltd. (Qingdao, China). *N*-Methylimidazole (99%) was obtained from Jiangsu Meihua Chemicals Co., Ltd. (Suzhou, China). The MWCNTs were obtained from Xiamen University, China, with diameters ranging from 15 to 45 nm and a surface area of 140 $m^2/g$. The MWCNTs were purified and converted into acid form via sonication in 1:3 concentrated nitric acid/sulfuric acid at 50°C for 4 h. The resulting solid was washed thoroughly with deionized water until the pH value was 6–7. 1-Chlorobutane (98%) and the other reagents were supplied from Sinopharm Chemical Reagent Co., Ltd. (Shanghai, China).

### Preparation of the ILs

For the HMImCl synthesis, an appropriate amount of HCl (36%) was added dropwise in a round-bottom flask containing *N*-methylimidazole in an ice bath. After it was stirred for several hours, the reaction mixture was evaporated *in vacuo*. The residue was washed with ethyl acetate and then dried by the azeotropic removal of water with a rotatory evaporator according to the literature to obtain the acidic IL HMImCl.[28]

BMImCl was prepared according to the literature.[29] Briefly, mixtures of 1-chlorobutane (1.2 mol), *N*-methylimidazole (1.0 mol), and $CH_3CN$ (150 mL) were added to a round-bottom flask fitted with a reflux condenser with stirring. After 48 h, the $CH_3CN$ was removed by distillation, and the residue was washed with ethyl acetate (3 × 60 mL) and then dried *in vacuo* at 100°C for 24 h to give the purified ILs.

### Preparation of the Chitosan/Cellulose/MWCNT Composite Membranes and Fibers

First, to obtain the mixed chitosan/cellulose/MWCNT ILs paste, we used a typical experimental procedure as follows:

1. Mixtures of chitosan (0.2 g) with BMImCl/HMImCl (9:1, w/w, 5 g) and of cellulose (0.6 g) with BMImCl (15 g) were independently heated at 100°C for 24 h with stirring to give clear liquids of chitosan (4 wt %) and cellulose (4 wt %), respectively.
2. The two liquids were mixed and heated at 100°C for 1 h with stirring to form a homogeneous chitosan/cellulose IL solution.
3. Various amounts of MWCNTs (8, 16, 24, 32, 40, 48, 56, and 64 mg) were suspended in BMImCl (1 g) and ground in an agate mortar for 5 min. The mixture continued to be ground for another 15 min after 20.8 g of a chitosan/cellulose ILs solution was added to the mortar, during which the suspension gradually turned into a glossy, black paste.

All processes were conducted under an infrared lamp because ILs absorb water easily. Second, some mixed paste was cast onto a glass plate. Then, the glass slide was soaked in a methanol bath to form membranes. The other mixed paste was transferred into a syringe, and then, the solution was injected into the methanol bath to form fibers. Last, after being soaked overnight to remove ILs, these regenerated membranes and fibers were oven-dried at 60°C. It is worth noting that the fibers needed to be wound on a glass bobbin to prevent recoiling.

### Measurements

**Fourier Transform Infrared (FTIR) Spectroscopic Analysis.** The FTIR study was carried out in the range 400–4000 $cm^{-1}$ with

spectroscopic KBr powder with an EXUS 670 instrument (Nicolet, Madison, USA).

**NMR.** The $^1$H-NMR (300-MHz) spectra of the ILs in $CDCl_3$ were recorded on a Bruker Advance DPX300 (Greifensee, Switzerland) at 25°C.

**Wide-Angle X-Ray Diffraction (WAXD).** WAXD measurements were conducted with a PW3040/60 X-ray diffractometer (PANalytical, Almelo, Netherlands) with Cu Kα radiation with the normal θ–2θ scanning method ($\lambda = 0.15418$ nm).

**Thermogravimetric Analysis (TGA).** TGA measurements were performed on a Netzsch STA 449 (Selb, Germany) at a heating rate of 10°C/min in nitrogen.

**Scanning Electron Microscopy (SEM).** The general morphologies were characterized by SEM (SEM LEO-1530, HITAchi, Tokyo, Japan) at an acceleration voltage of 5 kV. The samples were deposited onto double-sided conductive carbon tape, which was then ultimately attached to the surfaces of SEM brass stubs. These samples were then conductively cast with gold by sputtering for 20 s to minimize charging effects under imaging conditions.

**Mechanical Performance.** The tensile strengths ($\sigma t$'s) were calculated by the following equations:

$$\sigma t = F/dm(\text{membrane}) \quad (1)$$

$$\sigma t = F/(\Pi r^2)\,(\text{fiber}) \quad (2)$$

where $F$ is the maximum capacity, which was carried out under the tensile mode by an electronic universal testing machine (WDS-5, Tianshui Hongshan Testing Machine Co. LTD, Tianshui, China) and at a tensile rate of 5 mm/min. The thickness of the membranes ($d$) and the diameter of the fibers ($r$) were measured by a vernier caliper (Meifang Electric and Mechanical Services LTD, Suzhou, China) (precision = 10 $\mu$m), $m$ is the width of the membranes, and Π is circular constant.

The elongation at break ($\delta$) was calculated by the following equations:

$$\delta = (\Delta L/L) \times 100\% \quad (3)$$

$$\Delta L = L\prime - L \quad (4)$$

where $L'$ is the breaking length after deformation and $L$ is the gauge length. Four parallel measurements were carried out for each sample at a temperature of 25°C.

**Electrical Conductivity.** The thicknesses of the membranes and fibers were measured as discussed previously. The electrical conductivity of the composites was measured at room temperature on an Agilent impedance/material analyzer (E4991, Agilent Technoligies, Santa Clara, USA) with a four-probe method.

## RESULTS AND DISCUSSION

### FTIR Spectral Analysis

In our previous study, by virtue of the IL dissolution method, the obtained chitosan membrane was very brittle as was the chitosan fiber. It is well known that blending and incorporation are common ways to improve biopolymer mechanical properties. When the weight ratio of chitosan to cellulose was greater than 1:2, it was difficult to get a stable membrane.[30] Additionally, the best loading of MWCNTs was 4 wt %; this was drawn from the following analysis. Therefore, unless otherwise noted, the chitosan/cellulose blended or chitosan/cellulose/MWCNT composite materials were prepared with a 1:3 ratio of chitosan to cellulose and a 4 wt % MWCNT loading.

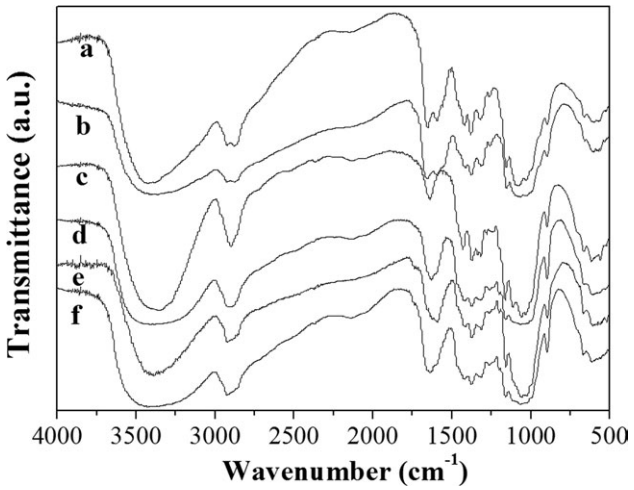


**Figure 1.** FTIR spectra of the (a) native chitosan, (b) regenerated chitosan, (c) native cellulose, (d) regenerated cellulose, (e) regenerated chitosan/cellulose, and (f) regenerated chitosan/cellulose/MWCNTs.

As shown in Figure 1, no FTIR spectrum for the ILs was observed; this indicated that the ILs were removed completely during the regeneration process. Compared with the FTIR spectrum of the original chitosan, the spectrum of regenerated chitosan changed little [Figure 1(a, b)]. There was no variable angle of $NH_3^+$ at 1520 $cm^{-1}$.[31] In our initial experiments, neither pure HMImCl nor its dilute aqueous solution could dissolve chitosan. This indicated that little or no ammonium salts came into being in our dissolution process. A plausible explanation was that the increase in the amount of $Cl^-$ improved the ability to dissolve chitosan because of the increased amount of HMImCl. The stretching vibration of N—H and O—H at about 3200–3500 $cm^{-1}$ [Figure 1(a–d)] and the bending vibration of N—H at about 1590 $cm^{-1}$ [Figure 1(a, b)] were weakened. The absorption band of the $CH_2$ scissoring motion at about 1425 $cm^{-1}$ was also weakened [Figure 1(a–d)].[32] This indicated that the H-bond networks in the native chitosan and cellulose were greatly destroyed by the ILs during the dissolution process, and the hydrogen bond network might not have been completely reconstituted during the regeneration process. It is worth noting that this weakening trend strengthened after the incorporation of MWCNTs [Figure 1(e, f)]. The MWCNTs might have been uniformly incorporated into the chitosan and cellulose; this would have resulted in the weakening trend.

### WAXD Analysis

Figure 2 shows the WAXD profiles of the natural chitosan, regenerated chitosan, natural cellulose, regenerated cellulose, regenerated cellulose/chitosan, and regenerated cellulose/chitosan/MWCNTs. The natural chitosan showed crystalline peaks around $2\theta = 10.1$ and 20.4°, which were assigned to the (020) and (100) reflections, respectively.[33] However, the regenerated chitosan only

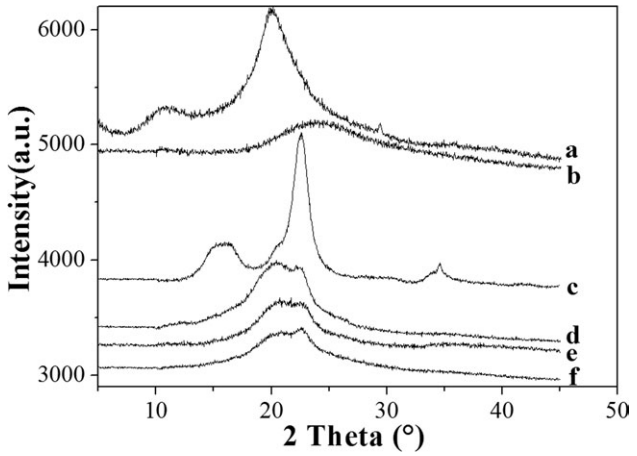


**Figure 2.** WAXD profiles of the (a) native chitosan, (b) regenerated chitosan, (c) native cellulose, (d) regenerated cellulose, (e) regenerated chitosan/cellulose, and (f) regenerated chitosan/cellulose/MWCNTs.

showed a broad amorphous halo centered at 25°. This indicated that during the dissolution process, BMImCl and HMImCl had broken intermolecular and intramolecular hydrogen bonds and destroyed the original crystalline form. The native crystal structure of chitosan was barely reconstituted and suffered a remarkable decrease in crystallinity. Similar trends were observed before and after cellulose regeneration. The natural cellulose exhibited crystalline peaks around $2\theta = 15.6$ and 22.6°, whereas the regenerated cellulose exhibited crystalline peaks around $2\theta = 20.3$ and 22.1°. This indicated that the transformation from cellulose I to cellulose II occurred after the dissolution and regeneration.[34] The diffraction peak intensity of the regenerated chitosan/cellulose decreased to a certain extent compared with that of the regenerated cellulose. This decrease in the crystallinity might have been caused by the weakened impact among cellulose chains due to the blending of chitosan. Furthermore, the diffraction peak intensity of the regenerated chitosan/cellulose decreased further after the incorporation of MWCNTs.

### TGA

The thermal decomposition of the chitosan/cellulose with different MWCNT contents is shown in Figure 3. Because the two biopolymers were similar, TGA showed one unique region of loss of mass. The incorporation of MWCNTs improved the thermal properties of chitosan/cellulose. The pure chitosan/cellulose material (membranes or fibers) began to lose weight at 291°C. In the case of the chitosan/cellulose/MWCNT composites containing 8 wt % MWCNTs, the onset of degradation was above 323°C; this was 32°C higher than that of the chitosan/cellulose blended material. On the other hand, the char yield of the composite materials increased with the incorporation of MWCNTs. At 500°C, the char yield of the chitosan/cellulose blended material was about 21.5%, whereas those of the composite materials containing 2 and 4 wt % MWCNTs were about 26.1 and 33.0%, respectively. This indicated that the char yield of the composite materials increased significantly with increasing appropriate amount of MWCNTs. However, in the case of an excessive amount of MWCNTs (>4 wt %), the char yield of the composite materials increased by the same amount of MWCNTs. For example, the composite material containing 8 wt % MWCNTs had a char yield of about 37.5% at 500°C.

### Morphological Observation

Chitosan/IL solutions were found to form a gel after being cooled down to room temperature. A brown gel was obtained after the ILs were extracted [Figure 4(a)]. Figure 4(b, d) shows the digital images of the chitosan/cellulose blended membrane and fibers. The membrane and fibers were brown; this indicated that chitosan blended into cellulose uniformly, and this was in agreement with the results of FTIR spectroscopy [Figure 1(e)] and WAXD [Figure 2(e)]. After the incorporation of the MWCNTs, the membrane and fibers turned black [Figure 4(c, e)].

The morphologies of the chitosan/cellulose/MWCNT composite materials were investigated by SEM. The free surface morphologies of the membrane and fibers were smooth [Figure 5(a, b)]; this indicated the good dispersion of chitosan in cellulose. Furthermore, no MWCNTs were found on the free surface of the membrane and fibers; this indicated that the MWCNTs were incorporated into the chitosan/cellulose blended matrix. Figure 5(c, d) shows typical fracture surfaces of the composite membrane and fiber after tensile tests. A uniform distribution of MWCNTs was observed, with some ends of the broken MWCNTs on the fracture surface of the membrane [the arrows point to them in Figure 5(c)] and some nanotubes of the nearly broken MWCNTs on the fracture surface of the fibers. These indicated that there was strong interfacial adhesion between the MWCNTs and chitosan/cellulose blended matrix. We concluded that both uniform dispersion and strong interfacial adhesion were key factors in the preparation of reinforcing nanocomposites, and this favored a more uniform stress distribution and minimized the presence of a stress concentration center.[35]

### Tensile Strength and Elongation Break Analysis

The tensile strength and elongation at break values of the chitosan/cellulose/MWCNT composite membranes and fibers with various MWCNT loadings are shown in Tables I and II and Figure 6. With increasing MWCNT loadings from 0 to 4 wt %,

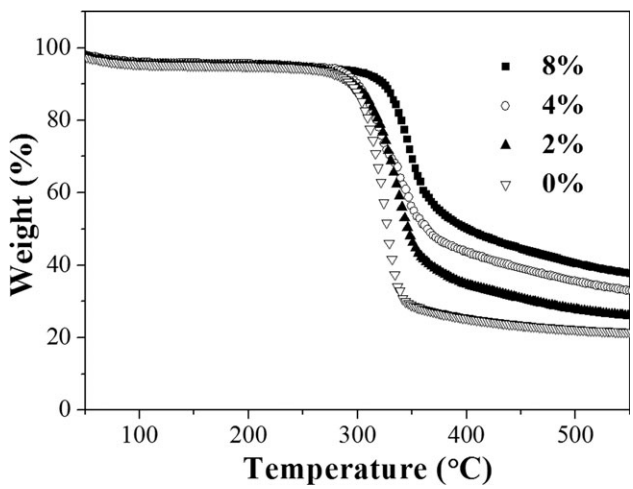


**Figure 3.** TGA curves of the chitosan/cellulose/MWCNT composite materials with various MWCNT loadings (Electrical Conductivity, $\sigma$).

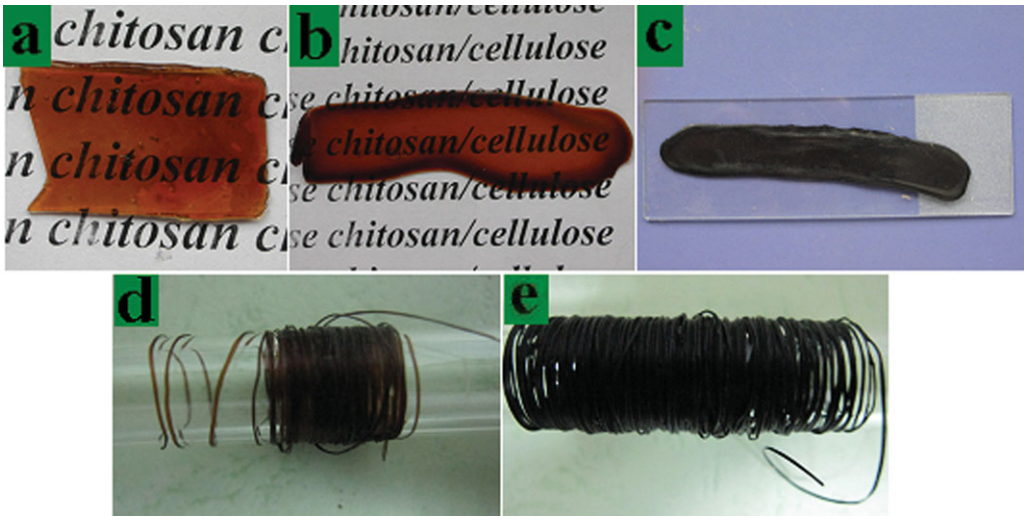


**Figure 4.** Digital images of the (a) regenerated chitosan gel, (b) regenerated chitosan/cellulose blended membrane, (c) regenerated chitosan/cellulose/MWCNT composite membrane, (d) regenerated chitosan/cellulose blended fibers, and (e) regenerated chitosan/cellulose/MWCNT composite fibers. [Color figure can be viewed in the online issue, which is available at wileyonlinelibrary.com.]

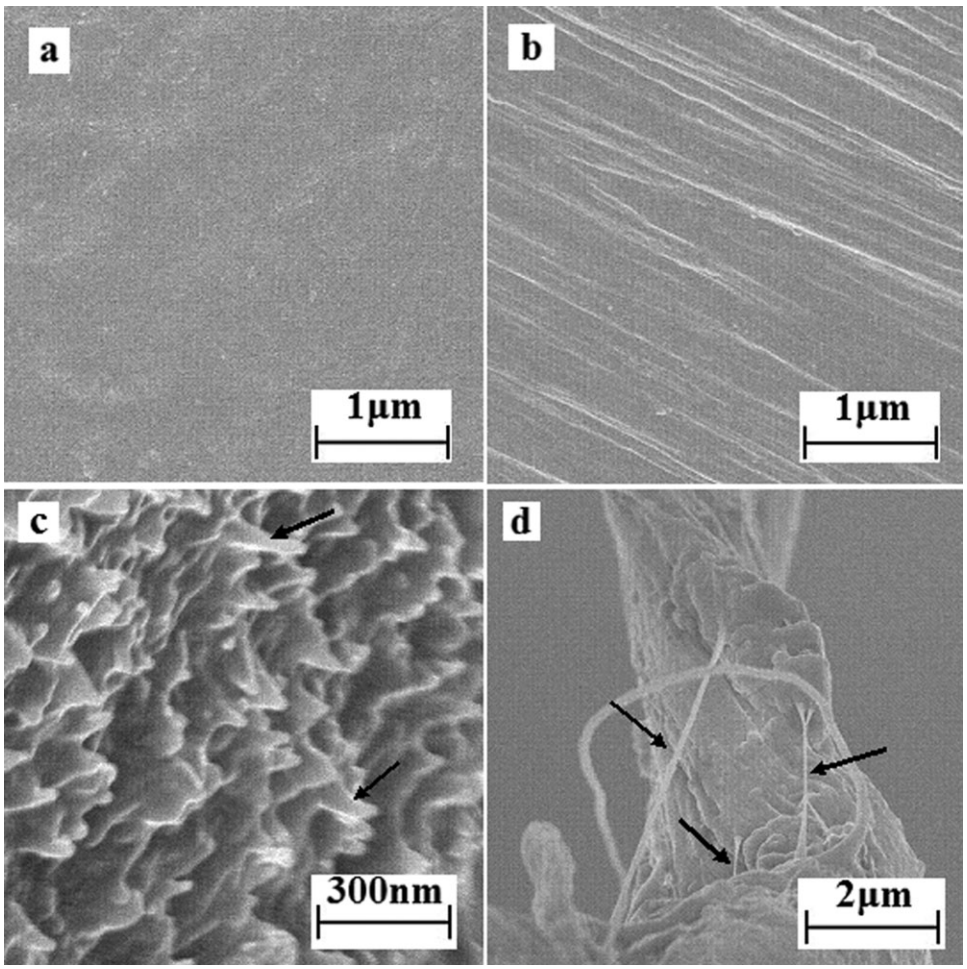


**Figure 5.** SEM micrographs of the free surfaces of the regenerated chitosan/cellulose/MWCNT composite (a) membrane and (b) fiber and the fracture surfaces of the regenerated chitosan/cellulose/MWCNT composite (c) membrane and (d) fiber.

Applied Polymer SCIENCE

**Table I.** Mechanical Performance of the Membranes

| MWCNT concentration (wt %) | *d* (mm) | *F* (N) | σt (MPa)[a] | *L′* (mm) | δ (%)[b] |
|---|---|---|---|---|---|
| 0 | 0.40 | 784.2 | 98 | 71.2 | 42.4 |
| 1 | 0.38 | 919.6 | 121 | 65.4 | 30.8 |
| 2 | 0.40 | 1104.1 | 138 | 60.9 | 21.7 |
| 3 | 0.37 | 1110.3 | 150 | 57.3 | 14.5 |
| 4 | 0.39 | 1263.6 | 162 | 55.0 | 10.2 |
| 5 | 0.36 | 1144.8 | 159 | 54.8 | 9.6 |
| 6 | 0.38 | 1086.9 | 143 | 54.4 | 8.9 |
| 7 | 0.37 | 932.4 | 126 | 54.0 | 8.1 |
| 8 | 0.37 | 791.8 | 107 | 53.8 | 7.7 |

[a] $m = 20$ mm.
[b] $L = 50$ mm.

the tensile strength of the composite membranes and fibers increased from 98 to 162 and 225 to 395 MPa, respectively. The increase in the tensile strength was saturated at a 4 wt % MWCNT loading. The tensile strengths of the membranes and fibers did not increase further with increasing MWCNT loadings greater than 4 wt %; this may have been caused by the aggregation of the MWCNTs at higher contents. Meanwhile, we concluded that the best loading of the MWCNTs was 4 wt %. On the other hand, the elongation at break of the membranes and fibers increased as the MWCNT loading increased; this indicated that the membranes and fibers became rigid. This may have been due to the rigidity of the MWCNTs and the interfacial adhesion between the MWCNTs and chitosan/cellulose blended matrix.

### Electrical Conductivity Measurements

The electrical conductivity of the chitosan/cellulose/MWCNT composite membranes was also measured. The composite membranes containing 4 wt % MWCNTs showed the highest electrical conductivity of $6.2 \times 10^{-3}$ S cm$^{-1}$ (Figure 7). Likewise, the

**Table II.** Mechanical Performance of the Fibers

| MWCNT concentration (wt %) | *r* (mm) | *F* (N) | σt (MPa) | *L′* (mm) | δ (%)[a] |
|---|---|---|---|---|---|
| 0 | 0.19 | 25.5 | 225 | 64.4 | 28.8 |
| 1 | 0.20 | 32.3 | 257 | 60.8 | 21.5 |
| 2 | 0.21 | 41.3 | 298 | 58.9 | 17.8 |
| 3 | 0.20 | 39.4 | 314 | 57.0 | 13.9 |
| 4 | 0.18 | 40.2 | 395 | 54.9 | 9.8 |
| 5 | 0.19 | 38.1 | 336 | 54.3 | 8.6 |
| 6 | 0.19 | 32.5 | 287 | 54.2 | 8.5 |
| 7 | 0.19 | 31.9 | 281 | 53.8 | 7.7 |
| 8 | 0.20 | 30.9 | 246 | 53.6 | 7.2 |

[a] $L = 50$ mm.

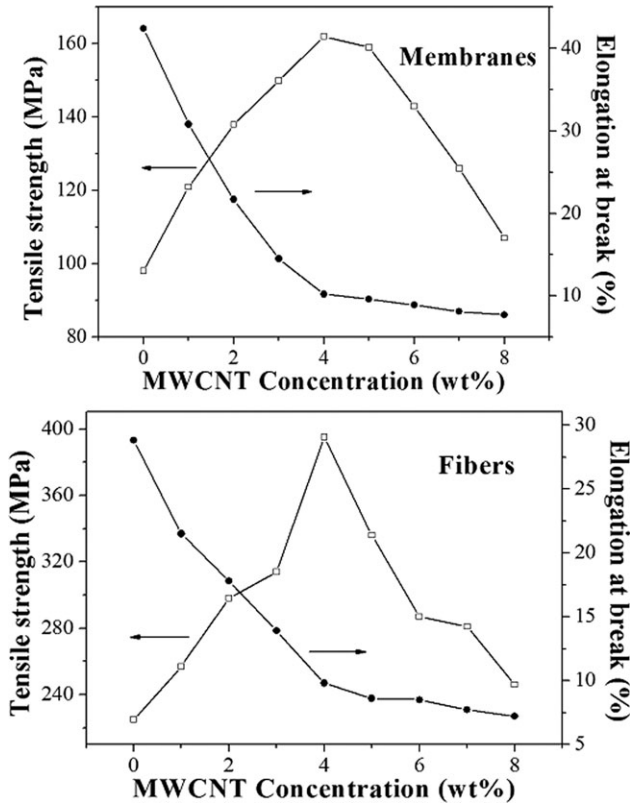


**Figure 6.** Tensile strength and elongation at break of the chitosan/cellulose/MWCNT composite membranes and fibers with various MWCNT loadings.

electrical conductivity did not increase further with increasing MWCNT loadings of greater than 4 wt %; this may have been due to the poor dispersion of the MWCNTs. These results were basically consistent with those reported in the literature.[36] All of the results of TGA and mechanical property and electrical conductivity measurement show that the best loading of MWCNTs was 4 wt %.

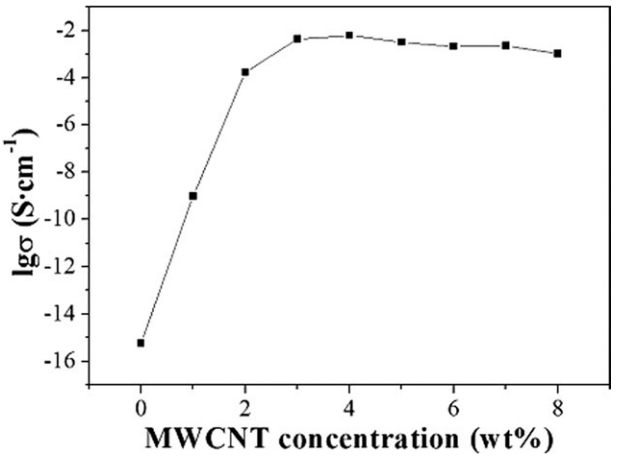


**Figure 7.** Electrical conductivity of the chitosan/cellulose/MWCNT composite membranes with various MWCNT loadings.

## CONCLUSIONS

With ILs as the solvent and dispersant, chitosan and cellulose were well dissolved, and the MWCNTs were well dispersed. The resulting mixed paste could be used to prepare chitosan/cellulose/MWCNT composite membranes and fibers by regeneration. The structure of chitosan and cellulose changed during the dissolution and regeneration processes. Because of the uniform dispersion and strong interfacial adhesion between the MWCNTs and chitosan/cellulose blended matrix, an appropriate amount of MWCNTs improved the thermal stability, mechanical properties, and electrical conductivity of the composite materials. Overall, this work provides a green method for preparing high-performance polymer nanocomposites with largely improved tensile properties.

## ACKNOWLEDGMENTS

The authors are grateful for the financial support from the National Natural Science Foundation of China (contract grant numbers 50873082 and 50903067) and the Zhejiang Provincial Natural Science Foundation of China (No. LY12B03001).

## REFERENCES

1. Jenkins, D. W.; Hudson, S. M. *Chem. Rev.* **2001,** *101*, 3245.
2. Cheng, M.; Deng, J.; Yang, F.; Gong, Y.; Zhao, N.; Zhang, X. *Biomaterials* **2003,** *24*, 2871.
3. Remuñán-López, C.; Bodmeier, R. *J. Controlled Release* **1997,** *44*, 215.
4. Welsh, E. R.; Schauer, C. L.; Qadri, S. B.; Price, R. R. *Biomacromolecules* **2002,** *3*, 1370.
5. Ravi-Kumar, M. N. V. *React. Funct. Polym.* **2000,** *46*, 1.
6. Park, W. H.; Jeong, L.; Yoo, D. I.; Hudson, S. *Polymer* **2004,** *45*, 7151.
7. Pei, H. N.; Chen, X. G.; Li, Y.; Zhou, H. Y. *J. Biomed. Mater. Res. A* **2008,** *85*, 566.
8. Caykara, T.; Alaslan, A.; Eroglu, M. S.; Güven, O. *Appl. Surf. Sci.* **2006,** *252*, 7430.
9. Thanpitcha, T.; Sirivat, A.; Jamieson, A. M.; Rujiravanit, R. *Carbohydr. Polym.* **2006,** *64*, 560.
10. Bourtoom, T.; Chinnan, M. S. *LWT-Food Sci. Technol.* **2008,** *41*, 1633.
11. Shih, C. M.; Shieh, Y. T.; Twu, Y. K. *Carbohydr. Polym.* **2009,** *78*, 169.
12. Yin, J.; Luo, K.; Chen, X.; Khutoryanskiy, V. V. *Carbohydr. Polym.* **2006,** *63*, 238.
13. Liu, T. X.; Phang, I. Y.; Shen, L.; Chow, S. Y.; Zhang, W. D. *Macromolecules* **2004,** *37*, 7214.
14. Park, J. H.; Jana, S. C. *Polymer* **2003,** *44*, 2091.
15. Yang, H.; Zhang, Q.; Guo, M.; Wang, C.; Du, R.; Fu, Q. *Polymer* **2006,** *47*, 2106.
16. Twu, Y. K.; Huang, H. I.; Chang, S. Y.; Wang, S. L. *Carbohydr. Polym.* **2003,** *54*, 425.
17. Baughman, R. H.; Zakhidov, A. A.; de-Heer, W. A. *Science* **2002,** *297*, 787.
18. Ke, G.; Guan, W.; Tang, C.; Guan, W.; Zeng, D.; Deng, F. *Biomacromolecules* **2007,** *8*, 322.
19. Gong, X.; Liu, J.; Baskaran, S.; Voise, R. D.; Young, J. S. *Chem. Mater.* **2000,** *12*, 1049.
20. Zhang, X.; Liu, T.; Sreekumar, T. V.; Kumar, S.; Moore, V. C.; Hauge, R. H.; Smalley, R. E. *Nano-Lett.* **2003,** *3*, 1285.
21. Fukushima, T.; Kosaka, A.; Ishimura, Y.; Yamamoto, T.; Takigawa, T.; Ishii, N.; Aida, T. *Science* **2003,** *300*, 2072.
22. Wu, Y.; Sasaki, T.; Irie, S.; Sakurai, K. *Polymer* **2008,** *49*, 2321.
23. Xie, H.; Zhang, S.; Li, S. *Green Chem.* **2006,** *8*, 630.
24. Swatloski, R. P.; Spear, S. K.; Holbrey, J. D.; Rogers, R. D. *J. Am. Chem. Soc.* **2002,** *124*, 4974.
25. Qin, Y.; Lu, X.; Sun, N.; Rogers, R. D. *Green Chem.* **2010,** *12*, 968.
26. Takegawa, A.; Murakami, M.; Kaneko, Y.; Kadokawa, J. *Carbohydr. Polym.* **2010,** *79*, 85.
27. Zhang, H.; Wang, Z.; Zhang, Z.; Wu, J.; Zhang, J.; He, J. *Adv. Mater.* **2007,** *19*, 698.
28. Ohno, H.; Yoshizawa, M. *Solid State Ionics* **2002,** *154*, 303.
29. Dyson, P. J.; Grossel, M. C.; Srinivasan, N.; Vine, T.; Welton, T.; Williams, D. J.; White, A. J. P.; Zigras, T. *J. Chem. Soc. Dalton Trans.* **1997,** *5*, 3465.
30. Xiao, W.; Chen, Q.; Wu, Y.; Wu, T.; Dai, L. *Carbohydr. Polym.* **2011,** *83*, 233.
31. Sashiwa, H.; Shigemasa, Y.; Roy. R. *Chem. Lett.* **2000,** 1186.
32. Higgins, H. G.; Stewart, C. M.; Harrington, K. J. *J. Polym. Sci.* **1961,** *51*, 59.
33. Tian, F.; Liu, Y.; Hu, K.; Zhao, B. Y. *J. Mater. Sci.* **2003,** *38*, 4709.
34. Raymond, S.; Kvick, A.; Chanzy, H. *Macromolecules* **1995,** *28*, 8422.
35. Coleman, J. N.; Khan, U.; Gunko, K. *Adv. Mater.* **2006,** *18*, 689.
36. Potschke, P.; Brunig, H.; Janke, A.; Fischer, D.; Jehnichen, D. *Polymer* **2005,** *46*, 10355.